View metadata, citation and similar papers at core.ac.uk

brought to you by CORE

provided by Elsevier - Publisher Connector

Cell, Vol. 119, 567–578, November 12, 2004, Copyright ©2004 by Cell Press

Magnitude of Binocular Vision Controlled by Islet-2 Repression of a Genetic Program that Specifies Laterality of Retinal Axon Pathfinding

Winnie Pak,[1] Robert Hindges,[1] Yoo-Shick Lim,[1] Samuel L. Pfaff,[2] and Dennis D.M. O'Leary[1,*]

[1]Molecular Neurobiology Lab
The Salk Institute
[2]Gene Expression Lab
The Salk Institute
La Jolla, California, 92037

Summary

Pathfinding of retinal ganglion cell (RGC) axons at the midline optic chiasm determines whether RGCs project to ipsilateral or contralateral brain visual centers, critical for binocular vision. Using *Isl2*$^{tau\text{-}lacZ}$ knockin mice, we show that the LIM-homeodomain transcription factor Isl2 marks only contralaterally projecting RGCs. The transcription factor Zic2 and guidance receptor EphB1, required by RGCs to project ipsilaterally, colocalize in RGCs distinct from Isl2 RGCs in the ventral-temporal crescent (VTC), the source of ipsilateral projections. *Isl2* knockout mice have an increased ipsilateral projection originating from significantly more RGCs limited to the VTC. *Isl2* knockouts also have increased *Zic2* and *EphB1* expression and significantly more Zic2 RGCs in the VTC. We conclude that Isl2 specifies RGC laterality by repressing an ipsilateral pathfinding program unique to VTC RGCs and involving Zic2 and EphB1. This genetic hierarchy controls binocular vision by regulating the magnitude and source of ipsilateral projections and reveals unique retinal domains.

Introduction

Neural systems are characterized by functional organizations established during development by mechanisms that specify classes of neurons and pathfinding by their axons. The interdigitation of eye-specific axon connections is a fundamental organization of the mammalian visual system (Reid, 2003). Eye-specific connections are formed initially through the direct projections of retinal ganglion cells (RGCs) to dorsal thalamus and midbrain and subsequently reiterated through higher order projections in neocortex. Eye-specific connections are patterned to segregate inputs from the two eyes, allowing them to be brought together in selective manners to generate binocular vision. The foundation for binocular vision is established during development by a critical pathfinding decision made by RGC axons at a midline choice point in the ventral diencephalon, resulting in the formation of the optic chiasm (OC) and the proper sorting of RGC axons to the left and right sides of the brain (Mason and Sretavan, 1997). RGC axons from the two eyes initially overlap in their targets but gradually segregate into eye-specific domains or layers (Godement et al., 1984) through a mechanism dependent upon patterned neural activity (Wong, 1999).

The crucial pathfinding decision of RGC axons at the OC has major functional consequences since it determines the proportion of RGCs that project ipsilaterally, and therefore the magnitude of binocular interactions, as well as the retinal source of ipsilaterally projecting RGCs, and therefore the part of retinotopic map and the visual field that participates directly in binocular vision. The relative size of contralateral versus ipsilateral projections varies across species and relates to the overlap in the visual fields of the eyes (O'Leary et al., 1983; Fukuda et al., 1989). The ipsilateral projection in mouse originates from the periphery of ventral-temporal (VT) retina, a region termed the VT crescent (VTC) that has binocular overlap of the visual field; contralaterally projecting RGCs are found throughout retina, including the VTC. In mice, 97%–98% of RGC axons project contralaterally and 2%–3% of RGCs project ipsilaterally (Drager and Olsen, 1980).

Axon guidance molecules, including slits (Plump et al., 2002) and ephrins (Nakagawa et al., 2000; Williams et al., 2003), influence RGC axon guidance at the OC and the OC's location along the ventral diencephalon. For example, when RGC growth cones pathfind at the OC, *ephrin-B2* is expressed by midline glia at the OC and an ephrin-B2 receptor, EphB1, is expressed by RGCs in the VTC. Blocking ephrin-B2 function in vitro decreases RGC axon repulsion by "OC" cells, and *EphB1*-null mice have a substantially diminished ipsilateral projection (Williams et al., 2003).

Studies of RGC laterality decisions at the OC suggested intrinsic factors that control an RGC axon's response to guidance molecules at the OC (Colello and Guillery, 1990; Godement et al., 1990; Marcus et al., 1995, 2000; Wang et al., 1995). However, a recent study of Mason and colleagues implicates for the first time the action of a specific regulatory gene, the zinc finger transcription factor (TF) Zic2, in determining RGC laterality (Herrera et al., 2003). In the RGC layer, *Zic2* expression is restricted to the VTC and is downregulated in RGCs coincident with their ipsilateral pathfinding decision at the OC. Mice hypomorphic for *Zic2* have a diminished ipsilateral projection, but expression of *Zic2* in the OC region and targets of RGCs complicates interpretations. However, in vitro, dorsal-temporal RGCs ectopically expressing *Zic2* have increased sensitivity to inhibitory influences of OC cells, whereas VTC RGCs transfected with blocking oligos to decrease *Zic2* expression extend longer axons. Together, these data provide compelling evidence that Zic2 activates an ipsilateral pathfinding program in RGCs (Herrera et al., 2003).

In a retinotopic mapping study, we showed that the LIM homeodomain (HD) TF, Isl2, is expressed by a subset of cells in the RGC layer (Brown et al., 2000). The spinal cord has been a prominent model for delineating functions of LIM-HD TFs, including specification of neuron identity and axon pathfinding (Jessell, 2000); for example, the Islet subfamily has a role in specifying the identity of visceral motor neurons (Thaler et al., 2004).

*Correspondence: doleary@salk.edu

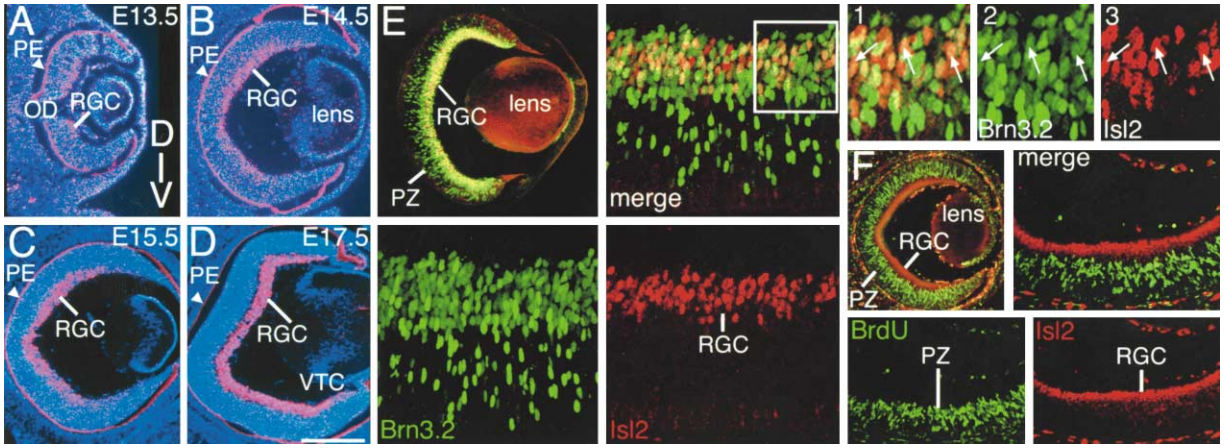

Figure 1. *Isl2* Expression in Embryonic Mouse Retina Is Limited to Postmitotic RGCs

(A–D) Coronal sections of retina at E13.5, E14.5, E15.5, and E17.5 after in situ hybridization with an S^{35}-labeled antisense probe against *Isl2* and stained with DAPI. Sections in (B)–(D) show temporal retina. *Isl2* is expressed in retinal ganglion cell (RGC) layer and has lower expression in the VTC, the origin of the ipsilateral projection (indicated in [D]).

(E and F) Immunostained coronal sections of E15.5 retina. Higher magnification panels show single channel and merged images. Double labeling for (E) the RGC marker, Brn3.2 (green) and Isl2 (red); (F) BrdU (green) and Isl2 (red); (E) Isl2-positive cells colocalize with Brn3.2-positive RGCs (arrows in numbered boxed regions).

(F) Isl2 RGCs are only present in the outer cell layer where differentiated RGCs are located, whereas BrdU-positive cells are located in the proliferative zone (PZ).

Abbreviations: D, dorsal; OD, optic disc; PE, retinal pigmented epithelium; V, ventral. Scale bar = 200 μm in (A)–(D), 250 μm in (E) and (F), 140 μm in (E), and 100 μm in (F) in higher magnification panels.

Here we address potential roles for Isl2 in specifying RGC identities, in particular the laterality of RGC projections, made possible by two lines of mice: a reporter line (*Isl2*^{tlacZ}) that selectively marks *Isl2*-expressing RGCs and their axons and a line with a targeted deletion of *Isl2*. We show that *Isl2* marks a subset of RGCs throughout the retina, including the VTC, that only projects contralaterally and that Zic2 and EphB1 colocalize in RGCs distinct from Isl2 RGCs. These findings suggest a role for Isl2 in specifying RGC laterality.

We confirm this role by showing that *Isl2*-null mice have an increased ipsilateral projection originating from significantly more RGCs limited to the VTC. The increased ipsilateral projection in *Isl2*-null mice correlates with increased expression of *Zic2* and *EphB1* and a significant increase in Zic2 RGCs in the VTC. We conclude that in a subset of VTC RGCs, Isl2 normally represses *Zic2* and *EphB1*, which are required for RGCs to project ipsilaterally. Our results define a genetic hierarchy that regulates the magnitude and source of ipsilateral retinal projections, forming the basis for binocular vision. In addition, our findings indicate that the retina is comprised of two genetically unique domains that reflect and determine the laterality of their projections to the brain.

Results

Isl2 Is Selectively Expressed by a Subpopulation of RGCs

In situ hybridization was used to analyze *Isl2* expression in mice from E12.5 to P8, focusing on retina and central visual pathways. *Isl2* expression is not detected in diencephalic or midbrain nuclei that receive retinal input, nor along the optic pathway, including the optic nerve (ON), OC, and optic tract (OT) (data not shown). In retina, expression is first detected at E13.5 in the outer layer of retina that contains the earliest generated retinal neurons, RGCs (Figure 1A). Thereafter, *Isl2* expression in retina remains limited to the RGC layer. At E14.5 and E15.5, *Isl2* expression exhibits a high-dorsal to low-ventral gradient (Figures 1B and 1C). Between E13.5 and E17.5, expression increases in peripheral retina. By E17.5, strong *Isl2* expression is seen throughout retina, with the exception of weaker expression in the VTC (Figure 1D). A similar pattern of *Isl2* expression is seen through P8 (data not shown). Double immunostaining shows that at least 94% of Isl2-positive cells colabel with the RGC marker, Brn3.2 (Xiang, 1998), indicating that essentially all Isl2 cells are RGCs (Figure 1E). About a third of RGCs are Isl2 positive, estimated by the ratio of cells double labeled with Isl2 and Brn3.2 to all Brn3.2-positive cells in the RGC layer (Figure 1E).

Double labeling using BrdU to detect proliferating cells and immunostaining for Isl2 shows that only postmitotic RGCs express *Isl2*. A single BrdU injection was given between E10.5 and E15.5; embryos were analyzed 1–2 hr later. Isl2 immunopositive cells are not detected at E10.5 to E12.5, but a high density of cells is labeled with BrdU (data not shown). Following a BrdU injection on E13.5 to E15.5, BrdU-labeled cells are localized deep in retina and Isl2-positive cells are preferentially found in the nascent RGC layer in outer retina and are not labeled with BrdU (Figure 1F).

To study the axonal projections of *Isl2* RGCs, we localized a tau-β-galactosidase (tau-β-gal) marker in *Isl2*^{tlacZ} mice targeted to the 3′-untranslated region of the *Isl2* gene, leaving Isl2 expression and function intact (Thaler et al., 2004). Coincident expression of functional Isl2 protein and the tau-β-gal marker was ensured by using

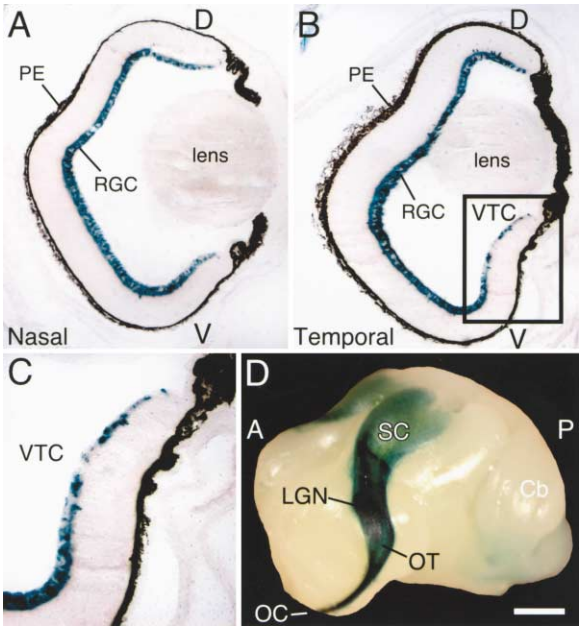

Figure 2. Selective Labeling of *Isl2*-Expressing RGCs and Their Axons in *Isl2*^{tlacZ} Mouse

(A–C) *Isl2* expression assayed by β-gal histochemistry in *Isl2*^{tlacZ} animals at postnatal day P2. Coronal sections through retina and subsequent X-gal staining show an even distribution of *Isl2* RGCs in nasal (A) and dorsal temporal retina (B). In contrast, the VTC (boxed in [B], higher magnification in [C]) shows diminished *Isl2* expression.

(D) Whole-mount β-gal histochemistry on a P5 *Isl2*^{tlacZ} brain reveals *Isl2* expression in the visual pathway. The tau-β-gal protein is preferentially targeted to axons, labeling the axonal projections of Isl2 RGCs throughout the optic pathway (cortex removed).

Abbreviations: A, anterior; Cb, cerebellum; D, dorsal; LGN, lateral geniculate nucleus; OT, optic tract; OC, optic chiasm; P, posterior; PE, retinal pigmented epithelium; RGC, retinal ganglion cells; SC, superior colliculus; V, ventral. Scale bar = 420 μm in (A) and (B), 220 μm in (C), and 500 μm in (D).

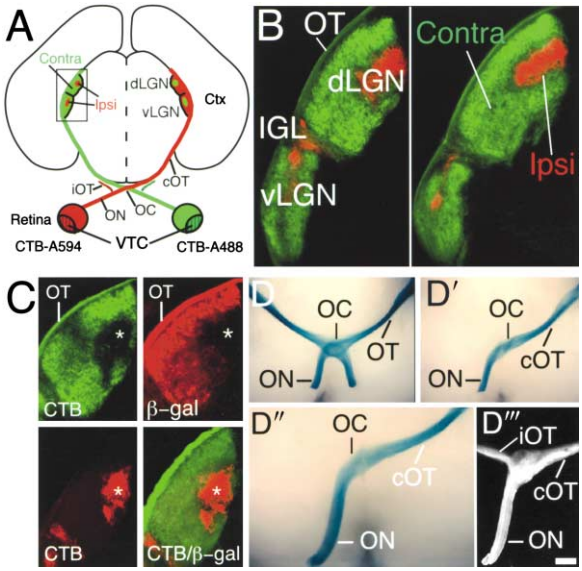

Figure 3. *Isl2*-Positive RGCs Project Only Contralaterally

(A) Schematic of the visual pathway from eyes to the lateral geniculate nuclei (LGN) labeled with two different colors. Hashed regions in retina depict the VTC (origin of the ipsilateral projection).

(B) Coronal sections through the LGN after double full eye fills at postnatal day P13 in wt mice. Innervation from both the contralateral (green) and ipsilateral eye (red) is visible.

(C) Coronal section of the dorsal LGN in *Isl2*^{tlacZ} mice at P13 doubly labeled with a single full eye fill, marking the entire contralateral-projecting RGC population (upper panel, green), and β-gal immunostaining marking specifically the *Isl2* axon projection (upper panel, red). The *Isl2* projection exhibits a similar staining pattern as the one from the contralateral eye, with the ipsilateral domain (asterisks) devoid of innervation. CTB fill of the ipsilateral projection (lower panel, red; asterisk) is distinct from the *Isl2* labeling with β-gal (green).

(D–D‴) Single eye enucleation studies in *Isl2*^{tlacZ}. The panels depict a ventral view of X-gal-stained optic chiasms from (D) unmanipulated, (D′) monoenucleated, and (D″ and D‴) monoenucleated mice after full eye fill of the remaining eye with CTB. The β-gal-positive axons from Isl2 RGCs only project into the contralateral optic tract (cOT) (D′ and D″); however, CTB-labeled RGC axons project into both the cOT and the ipsilateral optic tract (iOT) (D‴).

Abbreviations: CTB, cholera toxin subunit B; Ctx, cortex; d, dorsal; IGL, intergeniculate leaflet; OC, optic chiasm; ON, optic nerve; v, ventral. Scale bar = 150 μm in (B) and (C), 600 μm in (D) and (D′), and 300 μm in (D″) and (D‴).

a bicistronic mRNA to facilitate independent translation of *Isl2* and *tau-lacZ* components of the transcript. Thus, in these mice all β-gal-positive retinal cells are Isl2 RGCs. In the RGC layer, a subpopulation of cells are heavily labeled with tau-β-gal and interspersed with unlabeled cells (Figures 2A and 2B) in a pattern identical to that obtained with in situ hybridization and immunolabeling for Isl2. In the VTC, the proportion of Isl2 RGCs is lower than elsewhere in retina (Figures 2B and 2C). The tau-β-gal protein intensely labels the axonal projections of Isl2 RGCs throughout the optic pathway (Figure 2D). These findings validate the *Isl2*^{tlacZ} mouse as a tool to study Isl2 RGCs and their axonal projections.

Isl2 Selectively Marks Contralaterally Projecting RGCs

In mice, the majority of RGCs project contralaterally, but a small ipsilateral projection arises from the VTC (Figure 3A). In the VTC, about 50% of RGCs project ipsilaterally, and the remainder project contralaterally (Drager and Olsen, 1980). The decreased density of *Isl2* RGCs in the VTC suggests that Isl2 might selectively mark contralaterally projecting RGCs. In mice, contralateral and ipsilateral projections to the LGN, the major diencephalic target of RGCs, initially overlap but segregate postnatally resulting by P6 in a hole in the contralateral projection occupied by the ipsilateral projection (Godement et al., 1984). This segregated binocular projection is revealed by filling the two eyes with distinguishable anterograde axon tracers, CTB conjugated to a red (Alexa 594) or green (Alexa 488) chromophore (Figures 3A and 3B).

β-gal immunostaining in *Isl2*^{tlacZ} mice after segregation of RGC projections into eye-specific domains reveals a hole in the staining pattern in the LGN that resembles the hole observed in the LGN contralateral to a single eye filled with an anterograde tracer (Figure 3C). This hole in the tau-β-gal-labeled projection of *Isl2* RGCs to the LGN correlates directly with the RGC projection labeled with CTB injected into the ipsilateral eye (Figure

3C). This finding suggests that *Isl2* RGCs only project contralaterally.

To confirm that *Isl2* RGCs only project contralaterally, we performed two sets of experiments. First, we analyzed the laterality of RGC projections in normal and unilaterally enucleated *Isl2*^{tlacZ} mice. Examination of the OC in X-gal stained normal *Isl2*^{tlacZ} mice shows strong β-gal labeling of both ONs and OTs (Figure 3D). However, filling only one eye with CTB labels a single ON and reveals the large projection into the contralateral OT and the small projection into the ipsilateral OT (data not shown). To demonstrate the laterality of *Isl2* RGCs, we removed one eye on P2 or P8 and 2 to 8 days later did X-gal histochemistry or immunostaining for β-gal to label selectively the projections of *Isl2* RGCs and filled the remaining eye with CTB to label the projections of all RGCs. Examination of wholemounts and sections of unilaterally enucleated *Isl2*^{tlacZ} mice reveals that β-gal-positive axons of *Isl2* RGCs cross the ventral diencephalon where the OC would normally form and project exclusively into the contralateral OT (Figures 3D′ and 3D″ and data not shown). In contrast, CTB labeling reveals both this large crossed retinal projection and the smaller retinal projection into the ipsilateral OT (Figure 3D‴). These anterograde labeling studies show that Isl2 selectively marks a subpopulation of contralaterally projecting RGCs.

In the second set of experiments, we used retrograde labeling of RGCs with rhodamine beads injected into the superior colliculus (SC) of *Isl2*^{tlacZ} mice. The SC was chosen because virtually all RGCs project to it. Examination of retinal flat mounts from *Isl2*^{tlacZ} mice processed for β-gal histochemistry reveals dense fascicles of axons extending from Isl2 RGCs toward the optic disk; the fascicles become progressively thicker centrally as more RGC axons contribute to them (Figure 4A). These axon fascicles cut in cross-section, as well as the Isl2 RGCs that give rise to them, are revealed by β-gal immunostaining of transverse sections through retinas from *Isl2*^{tlacZ} mice (Figures 4B and 4C). A proportion of the β-gal-positive Isl2 RGCs throughout contralateral retina are labeled with rhodamine beads (Figure 4C). However, in retina ipsilateral to the injected SC, bead-labeled RGCs are only found in the VTC and all are singly labeled with either rhodamine beads or β-gal (Figure 4D). These studies show that Isl2 marks a subpopulation of contralaterally projecting RGCs throughout retina, including the VTC, and that Isl2 does not mark ipsilaterally projecting RGCs.

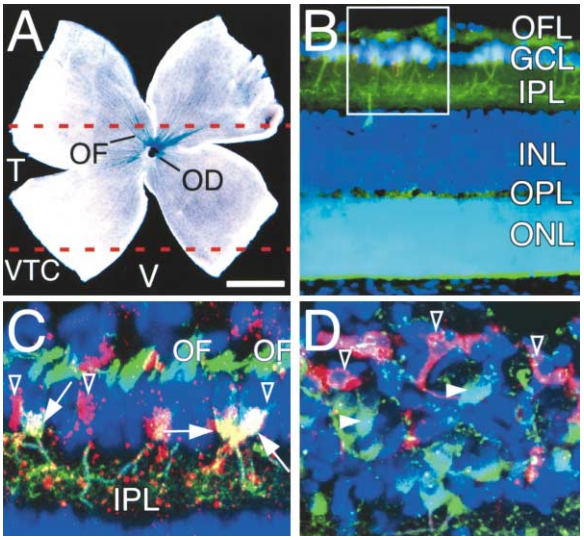

Figure 4. Ipsilaterally Projecting RGCs Do Not Overlap with *Isl2*-Positive RGCs

Flat mount of an X-gal-stained *Isl2*^{tlacZ} retina showing fascicles (OF) of β-gal-positive axons of Isl2 RGCs coursing through the optic fiber layer (OFL) to the optic disc (OD). A diminished number of β-gal-positive axons originating from the ventral temporal quadrant of retina is evident, due to the decreased number of Isl2 RGCs in the VTC. The OF become progressively thicker more centrally in retina as more β-gal-positive axons join them. Dashed lines represent the dorsoventral position of cross-sections shown in (C) (top line) and (D) (bottom line).

(B–D) Cross-sections through retinas from *Isl2*^{tlacZ} animals at postnatal day P10. RGCs are labeled retrogradely with rhodamine beads (red) injected into the superior colliculus, and Isl2 RGCs are labeled with a β-gal antibody (green). Sections are counterstained with DAPI (blue) to visualize cell nuclei.

(B) Low magnification view depicts layers in retina; boxed region represents layers shown in (C) and (D).

(C) High magnification of a retina contralateral to the bead injection: retrograde bead labeling in Isl2-positive RGCs (arrow) as well as in Isl2-negative RGCs (open arrowhead) is detectable. Large green profiles superficially are OFs of β-gal-positive axons of Isl2-expressing RGCs coursing through the OFL, cut in cross-section.

(D) High magnification of a retina ipsilateral to the bead injection. In the VTC no double labeled RGCs are detected, i.e., RGCs with red bead labeling (open arrowhead) do not overlap with green-labeled β-gal-positive Isl2 RGCs (solid arrowhead). Large OFs of β-gal-positive axons as in (C) are not seen because this section is from peripheral retina. Similar results are obtained in *Isl2*^{tlacZ} mice injected and examined at earlier postnatal ages.

Abbreviations: GCL, ganglion cell layer; INL, inner nuclear layer; IPL, inner plexiform layer; OD, optic disk; ONL, outer nuclear layer; OPL, outer plexiform layer; T, temporal; V, ventral. Scale bar = 750 μm in (A), 50 μm in (B), and 20 μm in (C) and (D).

Onset of Isl2 Expression in the VTC and Relationship between Isl2, Zic2, and EphB1-Positive RGCs

Zic2 and EphB1 expressed by RGCs in the VTC control their decision to project ipsilaterally at the OC; mice hypomorphic for *Zic2* (*Zic2*$^{kd/kd}$) or deficient for *EphB1* have substantially diminished ipsilateral projections (Herrera et al., 2003; Williams et al., 2003). Based on our findings above and roles for Isl2 in specifying subtypes of spinal motor neurons (Thaler et al., 2004), we hypothesize that Isl2 specifies the laterality of projections of a class of RGCs and their axon pathfinding decision at the OC by repressing an ipsilateral growth program potentially involving Zic2 and EphB1. Therefore, we examined the timing of Isl2 expression in the VTC relative to Zic2 and whether or not Isl2-, Zic2-, and EphB1-positive RGCs are distinct or overlapping.

We first examined the timing of *Isl2* expression, specifically its onset in the RGC layer of the VTC, using in situ hybridization (Figure 5) and immunostaining (data not shown), which yielded similar findings. *Isl2* expression is first detected in the VTC at E13.5, but compared to more central retina, expression is weak (data not shown). By E14.5, moderate levels of *Isl2* expression are detected in the VTC, and dense clusters of silver grains indicate that a proportion of VTC RGCs express *Isl2*

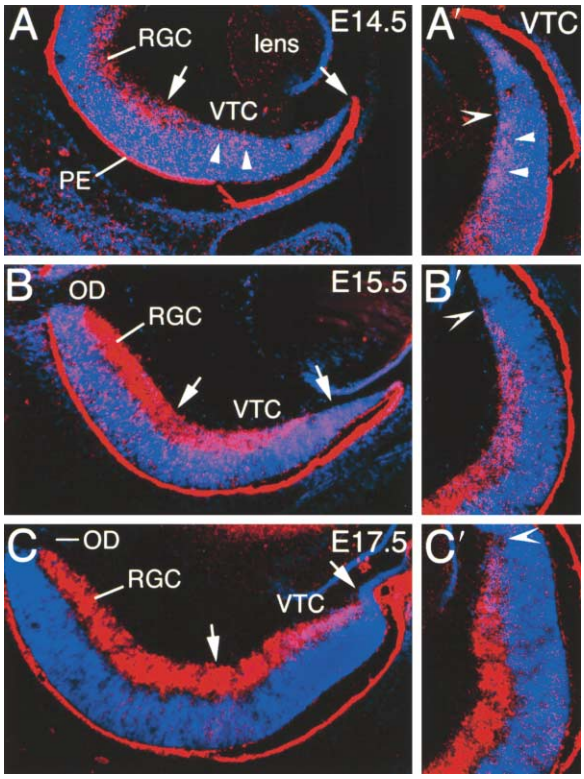

Figure 5. Onset of *Isl2* Expression in the VTC

Coronal sections of retina after in situ hybridization with an S^{35}-labeled antisense probe against *Isl2* (counterstained with DAPI) showing expression at E14.5 (A), E15.5 (B), and E17.5 (C). (A)–(C) show the ventral temporal half of retina; (A′)–(C′) show a higher magnification view of the periphery including VTC (arrows, [A]–[C]). *Isl2* expression is evident in RGC layer of the VTC at each age. Arrowheads in (A) and (A′) mark clusters of silver grains overlying cells in the RGC layer of the VTC. The convex arrowheads in (A′)–(C′) mark the peripheral end of the RGC layer abutting the ciliary margin. Abbreviations: OD, optic disc; PE, pigmented epithelium. Scale: 0.6 cm = 200 μm in (A)–(C) and 160 μm in (A′)–(C′).

(Figures 5A and 5A′). *Isl2* expression in the RGC layer of the VTC increases at E15.5 (Figures 5B and 5B′) and E17.5 (Figures 5C and 5C′). Herrera et al. (2003) report that Zic2-positive cells are first detected in small numbers in the VTC at E14.5, peak in number around E16.5, and are reduced in number by E18.5. Thus, onset of *Isl2* expression is similar to that of Zic2 and is appropriate to control pathfinding decisions by RGC axons at the OC.

If Isl2 functions in laterality decisions by repressing Zic2 and EphB1, we would expect that Isl2 is expressed in a subpopulation of RGCs distinct from those that express Zic2 and EphB1, whereas Zic2- and EphB1-expressing RGCs likely overlap. To address these issues, we performed immunostaining in wild-type (wt) and *Isl2*-null retina at E15.5, E16.5, and E17.5, using antibodies specific for Isl2 (Thaler et al., 2004) and Zic2 (Brown et al., 2003); to detect EphB1-positive RGCs, we used β-gal immunostaining in heterozygous *EphB1* knockout mice in which exon 3 is replaced with *lacZ* (Williams et al., 2003).

We find that 100% of Zic2-positive cells in the RGC layer colabel with the RGC marker, Brn3.2, indicating that all are RGCs (Figure 6A). At E17.5, counts in the region of overlap between Isl2 and Zic2 RGCs in the VTC show that the two subsets of RGCs are entirely distinct (Figure 6B). Similarly, Isl2 RGCs are entirely distinct from those that express EphB1 in the VTC, where EphB1 expression is high; in more central retina, where the density of EphB1 RGCs is low at these ages, Isl2 RGCs are also entirely distinct from EphB1 RGCs (Figure 6C). In contrast, in the VTC, 89% of Zic2 RGCs colabel for EphB1, indicating a near-complete overlap between the two populations (Figure 6D). These findings are consistent with a mechanism in which Isl2 controls the laterality of RGC projections by repressing *Zic2* and/or *EphB1*.

Isl2-Null Mice Have an Increased Ipsilateral Projection

To assess Isl2 function in controlling the laterality of RGC projections, we analyzed mice with a null mutation in the *Isl2* gene (Thaler et al., 2004). Analyses were done on P0 or earlier because essentially all *Isl2*-null pups die within 24 hr of birth. Histological examination of retina at embryonic ages and P0 and apoptotic cell death monitored by TUNEL staining at P0 during the peak of RGC cell death (Erkman et al., 2000) reveal no differences between wt and *Isl2*-null littermates (data not shown). In addition, the cross-sectional areas of transverse sections through the ON, a reliable indicator of the number of RGCs and their axons (O'Leary et al., 1986), show no difference between wt and *Isl2*-null littermates at E16.5 and P0 (data not shown). These findings indicate that *Isl2* mutants have a normal number of RGCs that extend axons through the ON to the brain.

To analyze potential alterations in the laterality of RGC projections, double anterograde axon labeling was done in P0 wt and *Isl2*-null littermates. Although P0 is before ipsilateral and contralateral projections segregate in the LGN, we were able to determine quantitatively the magnitude of the ipsilateral projection. In wt, the two eye injections label a large contralateral projection to the LGN (Figure 7A) and a small ipsilateral projection (Figures 7A′ and 7A″). In *Isl2* mutants, RGC axons are restricted to their normal pathways and targets, and a large contralateral projection to the LGN is observed (Figure 7B and data not shown). However, the ipsilateral projection to the LGN is substantially increased in *Isl2* mutants relative to wt (Figures 7B′ and 7B″).

We carried out two independent quantitative measurements of the ipsilateral projection to the LGN in wt and *Isl2*-null littermates: a "pixel intensity" analysis and a "signal threshold" analysis (see Experimental Procedures); each show that *Isl2*-null mice have a significantly increased ipsilateral projection. For the pixel intensity analysis, we measured the density of anterograde labeling of the ipsilateral projection to the LGN by quantifying the total pixel intensity corrected for background signal (Figure 7C). On average, the total pixel intensity in *Isl2* mutants ($n = 6$) is significantly increased by 60% compared to wt littermates ($n = 6$; $p < 0.01$, Student's t test). The total pixel intensity is greater in every *Isl2* mutant than in the wt with the highest level of labeling, indicating that the increased ipsilateral projection is present in each *Isl2* mutant analyzed.

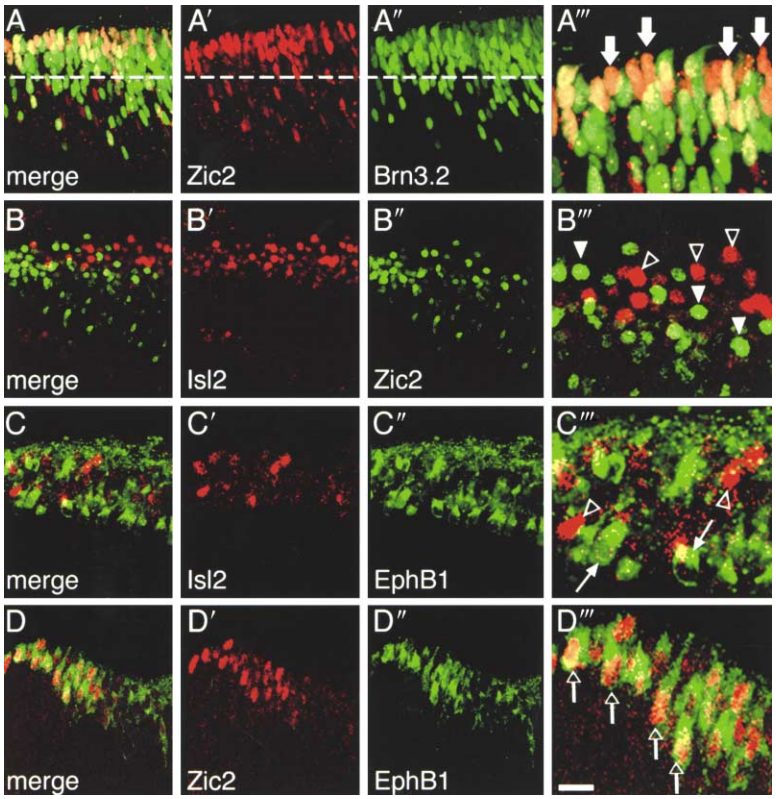

Figure 6. Zic2 RGCs Colocalize with EphB1, but Isl2 RGCs Are Distinct from RGCs Positive for Zic2 and EphB1

Coronal sections of through the VTC of E15.5, E16.5, and E17.5 retina after immunohistochemistry with combinations of antibodies specific for Isl2, Zic2, Brn3.2, and β-gal (for EphB1), shown in single channels, merged, and higher power.

(A–A‴) E16.5 Zic2-positive cells (red [A′]) colabel with RGC marker Brn3.2 (green [A″]; thick arrows [A‴]).

(B–B‴) E17.5 Isl2-positive (red [B′]; hollow arrowheads [B‴]) and Zic2-positive (green [B″]; white arrowheads [B‴]) RGCs are distinct populations (B‴).

(C–C‴) E17.5 Isl2-positive RGCs (red [C′]; hollow arrowheads, [C‴]) and EphB1-positive (green [C″]; arrows [C‴]) cells are also distinct populations (C‴).

(D–D‴) However, Zic2 (red [D′]) and EphB1 (green, [D″]) mark the same RGCs (arrows [D‴], E15.5). See Experimental Procedures for counts and ratios data and EphB1 localization.

Scale bar = 20 μm in higher magnification panels and 50 μm for all others.

We also performed a signal-threshold analysis of the proportion of pixels above background. We used the full range of factors to define a pixel as "signal," from a minimum value to define signal, i.e., 2× above background, to a maximum value of 5× above background, at which the percentage of pixels that exceeds the threshold for signal approached 0 in wt. Regardless of the factor used, the mean signal for *Isl2* mutants is significantly greater than that for wt (Figure 7D; for all factors $p < 0.05$). In summary, two independent quantitative measurements show that the ipsilateral projection is significantly increased in *Isl2* mutants, indicating that Isl2 has a role in specifying the laterality of RGC projections.

Significantly More RGCs Project Ipsilaterally in Isl2-Null Mice but Remain Restricted to the VTC

Because *Isl2* RGCs are found across the entire retina, it is possible that the increased ipsilateral projection in the *Isl2* mutants is due to an abnormal contribution from RGCs outside the VTC. To determine the distribution and number of RGCs that contribute to the ipsilateral projection in *Isl2*-null mice compared to wt, we retrogradely labeled RGCs by injections of DiI made unilaterally into anterior SC in P0 wt and *Isl2*-null littermates (Figures 8A–8C). Analyses of retinal wholemounts show a high density of retrogradely labeled RGCs throughout the contralateral retina in both wt and *Isl2* mutants, except the VTC, which has a lower density (data not shown). In retina ipsilateral to the injected SC, retrogradely labeled RGCs are almost exclusively restricted to the VTC in both wt ($n = 17$) and *Isl2* mutants ($n = 17$) (Figures 8D and 8E). Double retrograde labeling using fluorescein and rhodamine beads injected into each SC at P0 shows that no RGCs are double labeled in either wt or *Isl2*-null retinas (data not shown), indicating that individual RGCs project only ipsilaterally or contralaterally.

Quantification of retrograde labeling of ipsilaterally projecting RGCs was done on the subset of cases that had a similar size and placement of SC injections (Figures 8B and 8C) and labeling density in the contralateral retina. Two distinct quantitative analyses were done on wholemount retinas from five wt and five *Isl2*-null P0 mice: an automated pixel intensity threshold analysis to determine the amount of retrograde labeling by quantifying the number of pixels above a background threshold level of labeling intensity (see Experimental Procedures) and manual counts of retrogradely labeled RGCs. The mean for pixel intensity threshold analyses of the contralateral retinas of wt and *Isl2* mutants was within 2% (difference not significant). In contrast, the mean number of pixels above threshold in the VTC of retinas ipsilateral to the SC injections in *Isl2* nulls (3542 ± 886) is significantly increased ($p < 0.05$) by 122% compared to wt (1593 ± 162) (Figure 8F). Similarly, the number of retrogradely labeled RGCs in the VTC of *Isl2* nulls (1028 ± 153) is significantly increased ($p < 0.05$) by 80% compared to wt (571 ± 103) (Figure 8G). These findings show that the increased ipsilateral projection in *Isl2* mutants originates from a significantly greater number of RGCs, but that they are limited to the VTC, as in wt.

VTC of *Isl2*-Null Retina Has Increased Expression of *Zic2* and *EphB1* and Significantly More Zic2 RGCs

Our findings suggest that Isl2 represses an ipsilateral axon pathfinding program that involves Zic2 and EphB1.

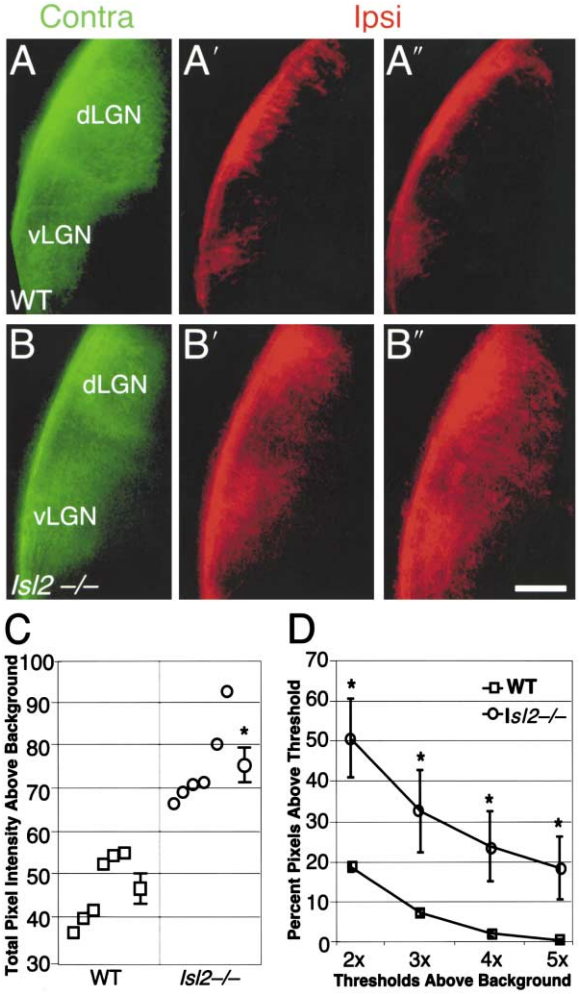

Figure 7. Ipsilateral RGC Projection Is Increased in *Isl2*-Null Mice

Coronal sections through the lateral geniculate nucleus (LGN) at postnatal day P0 after double full eye fills with two colors in wt (A–A″) and *Isl2*$^{-/-}$ mice (B–B″). Sections are shown in caudal to rostral order; dorsal is up. *Isl2*$^{-/-}$ mice show an increased ipsilateral projection to the LGN (B′–B″) compared to wt (A′–A″).

(C–D) Quantification of expanded LGN using two different methods.

(C) Total pixel intensity: individual cases are plotted, along with mean and standard error of the mean (SEM) for wt (square) and *Isl2*$^{-/-}$ (circle); all *Isl2*-null mice have a significantly higher total pixel intensity compared to wt, with no overlap between the two populations ($n = 6$, $p < 0.01$).

(D) Percentage of pixels above maximum range of threshold factors: pixel percentages are plotted at 2–5 times greater than background level; *Isl2*$^{-/-}$ percentages are higher than wt, independent of threshold level selected ($n = 6$, $p < 0.05$). See Experimental Procedures for methods.

Abbreviations: d, dorsal; v, ventral. Scale bar = 200 μm.

To address this issue more directly, we analyzed expression of *Zic2* and *EphB1* in wt and *Isl2*-null littermates at E15.5 and E17.5, complemented with counts of Zic2-positive RGCs in wt and *Isl2*-null littermates at E16.5 and E17.5.

In wt retina at E15.5 and E17.5, *Zic2* expression is confined to the VTC (Figures 9A and 9A′). In *Isl2*-null littermates, *Zic2* expression is also confined to the VTC but is at a higher level than in wt (Figures 9B and 9B′). In wt at E15.5 and E17.5, *EphB1* exhibits a moderate expression in the periphery of the RGC layer of VT retina in a domain similar to that of *Zic2* in the VTC and low expression across the rest of retina (Figures 9C and 9C′ and data not shown). In *Isl2*-null littermates, *EphB1* is expressed in the VTC at a higher level than in wt (Figures 9D and 9D′). Outside the VTC, *EphB1* expression is also elevated in the rest of retina in *Isl2*-null mice.

To complement these expression analyses, we determined the numbers and distributions of Zic2-positive RGCs using immunostaining on retinal sections from E16.5 and E17.5 wt and *Isl2*-null littermates. Qualitatively, Zic2-positive RGCs in *Isl2*-null retina have a similar distribution to wt, limited to the VTC, but are at a higher density. The number of Zic2-positive RGCs is significantly increased by about 50% in *Isl2*-null retina compared to wt at E16.5 ($p < 0.05$) and by about one-third at E17.5 ($p < 0.05$; see Experimental Procedures and Figure 9). The increased number of Zic2 RGCs, and the increased expression of *Zic2* and *EphB1* in the VTC of *Isl2*-null retina, provide genetic and cellular mechanisms to account at least in part for the increased ipsilateral projection in *Isl2*-null mice. These findings support a model in which Isl2 represses *Zic2* and *EphB1* and regulates the magnitude of the ipsilateral projection.

Statistical analyses of the distributions of Zic2 RGCs at E17.5 show that despite their increased number in *Isl2*-null retina, the peripheral to central extent of their distribution is not expanded compared to wt (Figure 9E), consistent with the distribution of retrogradely labeled, ipsilaterally projecting RGCs at P0 (Figures 8D and 8E). This latter finding suggests that the VTC is a genetically distinct part of retina and that retina is comprised of two unique domains, the VTC and the rest of retina.

Discussion

Isl2 Selectively Marks Contralaterally Projecting RGCs and Specifies Laterality Pathfinding Decisions by VTC RGCs

The goal of this study was to define genetic mechanisms autonomous to RGCs that specify the laterality of their axonal projections to the brain. The laterality of RGC axons results from their pathfinding decision at the midline OC that determines the magnitude and source of the ipsilateral retinal projection to the brain, forming the primary basis for binocular vision. Our findings demonstrate a prominent role for Isl2 in specifying RGC laterality.

In mice, the majority of RGC axons projects to contralateral visual centers in the brain, with ipsilaterally projecting RGCs limited to the VTC. We show that *Isl2* is expressed by a subpopulation of RGCs distributed across the entire retina, including the VTC. Analyses of *Isl2*^{tlacZ} mice in which Isl2 RGCs and their axons are selectively labeled reveal that Isl2 RGCs, including those in the VTC, project only to contralateral visual targets. We show that in the VTC, the TF Zic2 and the guidance receptor EphB1, which are required for RGCs to project ipsilaterally (Herrera et al., 2003; Williams et al., 2003), colocalize in a subset of RGCs distinct from Isl2 RGCs and that the onset of *Isl2* expression is similar to that of Zic2. Our analyses of *Isl2*-null mice reveal a substantially increased ipsilateral projection, arising from significantly more RGCs limited to the VTC (Figure 10A). Con-

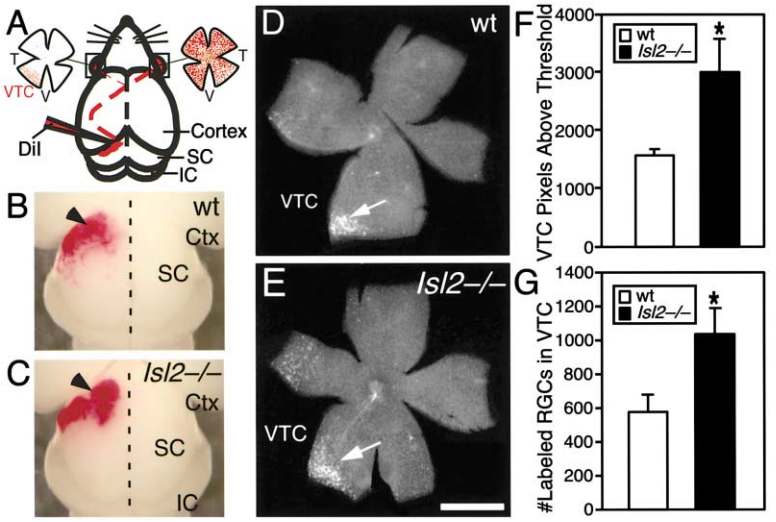

Figure 8. Increased Ipsilateral Projection in *Isl2*-Null Mice Originates from a Significantly Greater Number of RGCs Limited to the VTC

(A) Schematic of retrograde labeling: injection site (DiI) in the superior colliculus (SC), pathway of the labeled RGC axons (red dashed line), contralateral retina, and ipsilateral retina with the VTC.

(B and C) Injection sites (arrowheads) in the SC in wt (B) and *Isl2*$^{-/-}$ (C) mice at postnatal day P0. Dashed lines indicate midline.

(D and E) Corresponding flat-mounted ipsilateral retina from wt (D) and *Isl2*$^{-/-}$ mice (E) showing the backfilled RGCs. In *Isl2*$^{-/-}$ retina, more cells are labeled compared to wt, but remain largely limited to the VTC (arrow).

(F) Histogram showing that the mean number of pixels above a background threshold level of retrograde labeling intensity in the VTC of *Isl2*$^{-/-}$ (black, n = 5) is significantly increased (by 122%, $p < 0.05$) compared to wt (white, n = 5).

(G) Histogram of number of ipsilaterally projecting RGCs retrogradely labeled in ipsilateral VTC of *Isl2*$^{-/-}$ (black, n = 5) and wt (white, n = 5). Mean number is significantly increased in *Isl2*$^{-/-}$ (by 80%, $p < 0.05$) compared to wt. Same cases are quantified in (F) and (G).

Abbreviations: Ctx, cortex; IC, inferior colliculus. Scale bar = 600 μm in (B) and (C) and 400 μm in (D) and (E).

sistent with these findings, Isl2-null retina has significantly more Zic2 RGCs than wt and, as in wt, are restricted to the VTC. These findings show that Isl2 has a prominent role in determining the laterality of RGC projections. Because *Isl2* is expressed by RGCs, but not along the visual pathway or in central targets of RGCs, Isl2 likely acts autonomously in RGCs to specify their laterality.

We draw two major conclusions from our findings: first, that Isl2 represses a genetic program unique to RGCs in the VTC that involves Zic2 and EphB1 and controls the pathfinding decision of RGC axons to project ipsilaterally at the OC, and second, that RGCs in the VTC have a unique competence to project ipsilaterally and are genetically distinct from RGCs in the rest of retina.

Complementary Laterality Phenotypes in *Isl2*, *Zic2*, and *EphB1* Mutants: Implications for a Genetic Hierarchy Regulating Midline Axon Pathfinding

Mice hypomorphic for Zic2 (*Zic2*$^{kd/kd}$ mice; Herrera et al., 2003) or null for EphB1 (Williams et al., 2003) have a substantially diminished ipsilateral projection (Figure 10A). The expression patterns of *Zic2* and *EphB1* are consistent with their proposed roles in controlling laterality decisions by axons of VTC RGCs. In the RGC layer, *Zic2* is only expressed in the VTC; Zic2-positive RGCs are first detected at E14.5, peak in number around E16.5, and by E18.5 are declining in number (Herrera et al., 2003). The downregulation of *Zic2* expression in VTC RGCs is coincident with the pathfinding decision of their axons at the OC. Although *Zic2* is also expressed in the pathway and targets of RGCs, including the OC, the overall data of Herrera et al. (2003) provide a compelling argument that Zic2 activates an ipsilateral pathfinding program in RGCs and its expression in RGCs is sufficient for them to project ipsilaterally, an interpretation strengthened by our findings.

At embryonic ages, *EphB1* is most highly expressed in the VTC (Williams et al., 2003). The similarities in laterality phenotypes in *Zic2*$^{kd/kd}$ and *EphB1* mutant mice and our demonstration that virtually all Zic2 RGCs are also EphB1 positive suggest that Zic2 positively regulates *EphB1*, resulting in high expression of *EphB1* in the VTC. It follows, then, that the decreased ipsilateral projection in *Zic2*$^{kd/kd}$ mice is due to diminished Zic2 activation of *EphB1*, resulting in reduced *EphB1* expression in VTC RGCs and fewer RGC axons repelled into the ipsilateral OT by ephrin-B2 at the midline OC (Figure 10B); however, changes in *EphB1* expression have not been reported in *Zic2*$^{kd/kd}$ mice.

Our findings indicate that Isl2 normally represses *Zic2* expression in RGCs in the VTC and either directly represses *EphB1* expression or indirectly through repression of *Zic2* and that the increased ipsilateral projection in *Isl2*-null mice is due to a loss of this repression and upregulation of Zic2 and EphB1 (Figure 10B). This model is consistent with several pieces of data. First is the timing of expression of Isl2 and Zic2 in VTC RGCs. The onset of *Isl2* expression in VTC RGCs is similar to that of Zic2: we detect weak *Isl2* expression in the VTC as early as E13.5, and moderate levels of *Isl2* expression are evident by E14.5, the age when Zic2 expression in VTC RGCs is first detected (Herrera et al., 2003). Second, Zic2 and EphB1 colocalize in a subset of RGCs distinct from Isl2 RGCs. Third, we find increased expression of *Zic2* and *EphB1* and a significant increase in Zic2-positive RGCs in the VTC of *Isl2*-null retina. Fourth, the laterality phenotype of *Isl2*-null mice complements that of *Zic2*$^{kd/kd}$ and *EphB1* mutants.

The first RGC axon growth cones reach the OC around E12.5, and a very small proportion project into the ipsilateral OT (Colello and Guillery, 1990; Godement et al., 1990; Sretavan, 1990; Plump et al., 2002). These early ipsilateral axons are transient and arise from RGCs in dorsal-central retina suggested to express EphB1 (Williams et al., 2003). We find that, as in the VTC, outside the VTC Isl2 RGCs and EphB1 RGCs are distinct populations in wt and that *Isl2* mutants have increased EphB1

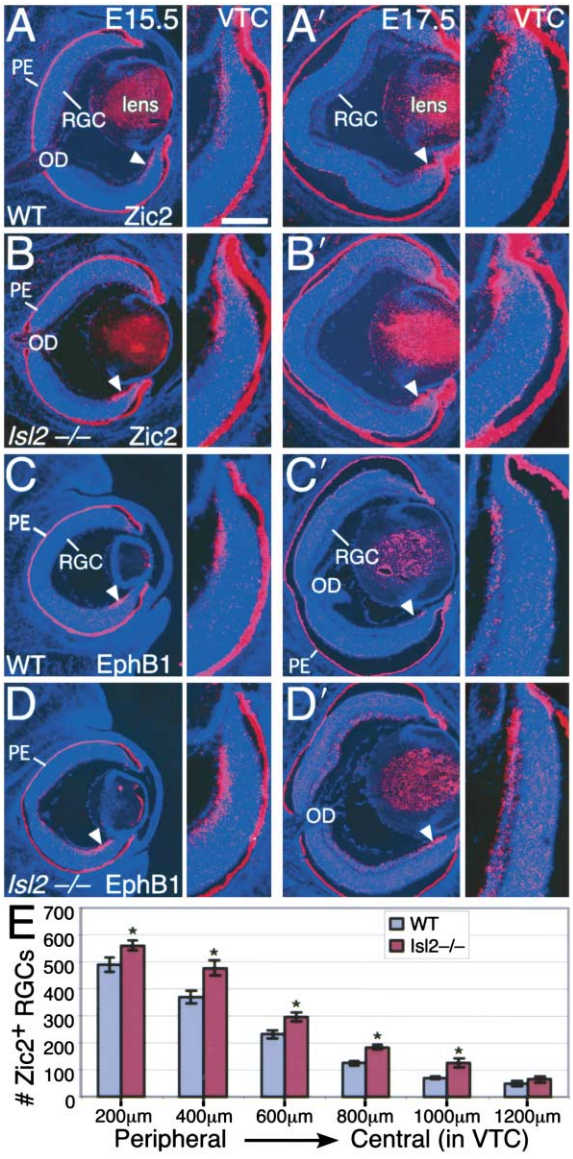

Figure 9. VTC of *Isl2*-Null Retina Has Increased Expression of *Zic2* and *EphB1* and Significantly More Zic2-Positive RGCs.

Coronal sections of E15.5 and E17.5 retina from wt (A and C) and *Isl2*$^{-/-}$ mice littermates (B and D) after in situ hybridization with S^{35}-labeled antisense probes against *Zic2* (A and B) and *EphB1* (C and D) stained with DAPI. Dorsal is up for all panels showing entire retina. Expression of *Zic2* in wt and *Isl2*$^{-/-}$ mice at E15.5 (A and B) and E17.5 (A′ and B′): in *Isl2*$^{-/-}$ mice, *Zic2* is upregulated exclusively in the VTC (arrowheads, higher magnification) at both developmental stages. Expression of *EphB1* in wt and *Isl2*$^{-/-}$ mice at E15.5 (C and D) and E17.5 (C′ and D′): in *Isl2*$^{-/-}$ mice, *EphB1* is strongly upregulated in the VTC and moderately in the RGC layer outside the VTC.

(E) Histogram of counts of Zic2-immunostained RGCs in peripheral ventral temporal retina of E17.5 wt (n = 4) and *Isl2*$^{-/-}$ (n = 4) mice binned according to the peripheral to central location. Significantly more Zic2 RGCs are found in each of the first five bins in *Isl2*$^{-/-}$ compared to wt (0–1000 μm; $p < 0.05$ for each bin). The number of Zic2 RGCs outside 1000 μm is not significantly different between wt and *Isl2*$^{-/-}$. At E17.5, the total number of Zic2 RGCs in *Isl2*$^{-/-}$ (1706 ± 100; n = 4) is significantly increased ($p < 0.05$) compared to wt (1334 ± 55; n = 4). See Experimental Procedures.

Abbreviations: OD, optic disc; PE, retinal pigmented epithelium. Scale bar = 400 μm in full retina panels and 160 μm in VTC magnifications.

expression outside the VTC. These findings indicate that Isl2 represses *EphB1* expression in a subset of RGCs throughout retina. Since *Zic2* is only expressed in VTC RGCs in wt and *Isl2* mutants, Isl2 can repress *EphB1* expression independent of its repression of *Zic2*. Further, because Zic2 RGCs are limited to the VTC (Herrera et al., 2003), it is likely that Zic2 is not required for *EphB1* expression outside the VTC (present study).

Ipsilaterally projecting RGC axons from the VTC reach the OC around E13.5 to E14.5 (Colello and Guillery, 1990; Godement et al., 1990; Sretavan, 1990; Sretavan and Reichardt, 1993; Marcus et al., 1995; Plump et al., 2002). In the VTC, only ipsilaterally projecting RGCs are generated at E11.5 and E12.5. Between E13.5 and E16.5, both ipsilaterally projecting and contralaterally projecting RGCs are generated in the VTC, whereas only contralaterally projecting RGCs are generated in the rest of retina (Drager, 1985). VTC RGCs generated on E11.5 and E12.5 must be Isl2 negative since they only project ipsilaterally. In contrast, RGCs born between E13.5 and E16.5 should be a mix of Isl2-positive RGCs and Zic2-positive RGCs because they project contralaterally and ipsilaterally, respectively. Therefore, based on the time of arrival of growth cones at the OC, the onset of *Isl2* expression, and the report that only later generated RGCs in the VTC project contralaterally, the increased ipsilateral projection in *Isl2*-null mice must be due to a change in the laterality of the pathfinding decision of later generated RGCs in the VTC that are Isl2 positive in wt mice.

Mouse Retina Is Comprised of Two Distinct Domains that Relate to Roles for Isl2 and Zic2 in Controlling RGC Laterality

Findings relating RGC birthdates to their laterality and the expression patterns of Isl2 and Zic2 suggest a model in which retina is comprised of two distinct domains of RGCs, an ipsilateral domain, i.e., the VTC, with a default mechanism to project ipsilaterally, and a contralateral domain comprised of the rest of retina that has a default mechanism to project contralaterally (Figure 10C). At E11.5 and E12.5, retina can be subdivided into two distinct domains based on differences in the generation of RGCs that will later project only ipsilaterally, the VTC, or contralaterally, the rest of retina (Drager, 1985).

Strong support for the concept that the VTC is a genetically distinct domain is that the increased numbers of Zic2 RGCs in *Isl2*-null retina have the same distributions as in wt, being restricted to the VTC. In addition, the increased ipsilateral projection in *Isl2*-null mice arises from a substantially increased number of RGCs, but again they appear to be limited to the VTC. Zic2 confers the default for VTC RGCs to project ipsilaterally. Other TFs likely act similarly to Zic2, at least for the earlier RGC laterality decisions at the OC because they are made before Zic2-positive RGCs are detected (Herrera et al., 2003). The expression of *Isl2* in a subset of later generated RGCs in the VTC—the majority of VTC RGCs are generated at E13.5 and later, after the onset of Isl2 expression—represses the default to project ipsilaterally, resulting in these RGCs to project contralaterally. Which TFs confer the default in the rest of retina to project contralaterally is unknown; Isl2 may be involved, but our findings show that it is not required since RGCs

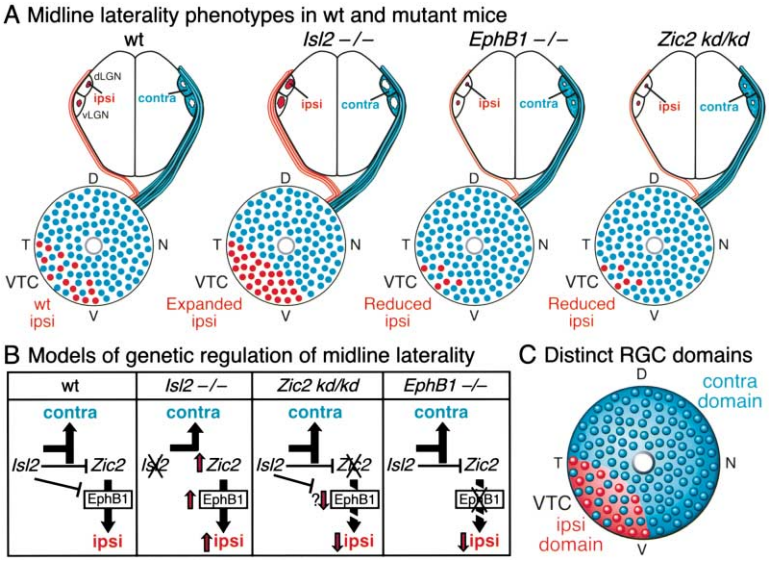

Figure 10. Proposed Genetic Hierarchy Controlling RGC Laterality and Model of Genetically Unique Domains in Retina

(A) In wt mice, ipsilaterally projecting RGCs are restricted to the VTC (red dots) whereas contralaterally projecting RGCs are found throughout retina, including the VTC. Isl2 RGCs account for one-third of all RGCs (blue dots), are distributed throughout retina, and only project contralaterally. *Isl2*$^{-/-}$ mice have a significantly increased ipsilateral projection arising from significantly more RGCs compared to wt, but they remain restricted to the VTC as in wt. In *Zic2* hypomorphic mice (*Zic2*$^{kd/kd}$), as well as in *EphB1*$^{-/-}$ mice, the ipsilateral projection is substantially reduced.

(B) Our findings show that in the VTC, *Isl2* represses an ipsilateral axon pathfinding program, which involves repression of *Zic2* as well as *EphB1*, either directly or through repression of *Zic2*. We conclude that in wt, Zic2 determines the source of the ipsilateral projection by activating an ipsilateral axon pathfinding program including EphB1, and Isl2 acts upstream to repress *Zic2* to determine the proportion of RGCs in the VTC that project ipsilaterally versus contralaterally. Isl2 repression of the ipsilateral RGC pathfinding program results in contralaterally projecting RGCs in the VTC. In the absence of Isl2, repression of *Zic2* and *EphB1* is eliminated, and additional RGCs in the VTC are Zic2 and EphB1 positive and project ipsilaterally. We predict that in *Zic2*$^{kd/kd}$ mice, the ipsilateral projection is diminished due to a reduction in its induction of EphB1. Our findings suggest that Isl2 is not required for RGCs to project contralaterally; the contralateral axon pathfinding program is specified by unknown regulatory proteins, but may be redundant with Isl2 in a subset of RGCs. Red arrows indicate increases (up) or decreases (down).

(C) Our findings suggest two genetically distinct domains in mouse retina: a domain with a default to project ipsilaterally, the VTC, and a domain comprised of the remainder of retina with a default to project contralaterally.

in the contralateral domain project contralaterally in *Isl2*-null mice.

Conclusions

The present study establishes a genetic hierarchy specifying RGC laterality and the control of RGC axon pathfinding at the OC. Our findings, together with those of Herrera et al. (2003), lead us to conclude that Zic2 determines the source of ipsilateral projections by activating an ipsilateral axon pathfinding program and that Isl2 acts upstream to repress *Zic2* to determine the proportion of RGCs in the ipsilateral source, the VTC, that project ipsilaterally versus contralaterally. Isl2 repression of *Zic2* and the ipsilateral RGC pathfinding program results in contralaterally projecting RGCs in the VTC. Through this hierarchical genetic interaction, the part of retinotopic map, and therefore the visual field, that participates directly in binocular vision and the degree of binocular interactions is regulated.

Experimental Procedures

Mice

Analyses were done blind to genotype and according to institutional guidelines and protocols. Morning of the vaginal plug is E0.5; the first neonatal day is P0. *Isl2*^{tlacZ} and *Isl2* knockout mice were made and genotyped as described (Thaler et al., 2004).

Microscopy

Digital images were obtained with a Zeiss LSM 510 confocal microscope, a Q-Imaging Retiga-EX digital camera on a Nikon Microphot-FX microscope, or a Zeiss SV Micro digital camera on a Zeiss SV11 dissecting microscope.

In Situ Hybridization

S^{35}-labeled and digoxigenin antisense riboprobes were synthesized from the following: full-length rat *Isl2* cDNA clone (1298 bp; Thaler et al., 2004), a 682 bp fragment (complete exon 3) of mouse *EphB1* cDNA (nucleotides 166–847, from M. Henkemeyer), and a 721 bp fragment of mouse *Zic2* cDNA (nucleotides 456–1176). In situ hybridizations were performed on 20 μm cryosections as described (Brown et al., 2000) and DAPI stained.

Immunohistochemistry, TUNEL, BrdU Labeling

E10.5–E16.5 mice were immersion fixed in 4% paraformaldehyde (PFA); E17.5 and older mice were perfused with PFA. Tissues were cryosectioned as described (Thaler et al., 2004). Primary antibodies for Isl2 (guinea pig, 1:8000 dilution; Thaler et al., 2004), Zic2 (rabbit, 1:20,000; Brown et al., 2003), Brn3.2 (goat, 1:200; Santa Cruz; Xiang, 1998), and β-gal (rabbit, 1:8000; Cappel) were visualized using species-specific secondary antibodies conjugated to Alexa-594 and Alexa-488 (Molecular Probes). To detect EphB1 RGCs, we used β-gal immunostaining in heterozygous mice in which exon 3 of EphB1 is replaced with *lacZ* (Williams et al., 2003). Apoptosis was assessed with the in situ cell death detection kit (Roche). BrdU was injected i.p. (10 μl/g weight); 1–2 hr later, mice were fixed and prepared for Isl2 immunohistochemistry. To detect BrdU, sections were refixed in 4% PFA, incubated in 2N HCl for 30 min at 37°C: primary BrdU antibody was applied (1:100, Accurate) and visualized with FITC-conjugated anti-rat secondary antibody (1:250, Jackson Laboratory).

Quantitation of Immunolabeled Cells

Immunolabeled cells were counted on sections and expressed as corrected absolute numbers or as percentages. To quantify Zic2 immunostained cells at E17.5, total numbers of labeled cells in the RGC layer were counted in every section through wt (n = 4) and *Isl2*-null (n = 4) retinas. Counts were corrected for double counting using a stereological correction factor N = (nT)/(T+D), where N is corrected number of cells, n is number of profiles (nuclei) counted, T is section thickness (18 μm), and D is average diameter of the labeled nucleus (Abercrombie, 1946; Guillery and Herrup, 1997). To

determine the percentage increase of Zic2-positive RGCs in *Isl2*-null versus wt at E16.5, Brn3.2-positive RGCs were localized in the RGC layer of the VTC and scored whether they were colabeled with Zic2; the proportion of colabeled RGCs was compared between genotypes. Zic2-positive cells were compared to Brn3.2-positive cells at E16.5 in the RGC layer of the VTC of wt and *Isl2*-null. Counts were done in two cases for each labeling combination: in wt, 42 Zic2 RGCs in a field of 209 Brn3.2 (20% Brn3.2-positive RGCs were also Zic2 positive); in *Isl2*-null, 66 Zic2 RGCs in a field of 207 Brn3.2 RGCs (32% Brn3.2-positive RGCs are also Zic2 positive).

For determining the percentage of cells colabeled using various antibody pairings in E17.5 wt, we randomly selected 100 cells immunolabeled with a given marker in the RGC layer of the VTC from multiple sections and retinas and determined whether they were labeled with the other marker. Cells were selected in the region of overlap of cells expressing the two proteins being analyzed. We also localized EphB1 RGCs outside the VTC and determined whether they colabeled with Isl2. Counts in the VTC were Isl2/Brn3.2, 100 Isl2 cells—94 colabeled with Brn3.2; Zic2/Brn3.2, 100 Zic2 cells—100 colabeled with Brn3.2; Isl2/Zic2, 100 Isl2 cells—0 colabeled with Zic2; Isl2/EphB1, 100 Isl2 cells—0 colabeled with EphB1; Zic2/EphB1, 100 Zic2 cells—89 colabeled with EphB1. All counts were done at E17.5, except Isl2/Brn3.2 done at E16.5. Counts outside the VTC were EphB1/Isl2, 34 EphB1 RGCs—0 colabeled with Isl2.

Other data and "n" values are presented in the text and figure legends. Statistical analyses were performed in Excel.

X-Gal Staining

Isl2^{tlacZ} mice were perfused with 4% PFA and brains processed for X-gal staining (BioVectra) at 30°C overnight. For retinal sections, heads were fixed, cryosectioned at 20 μm, stained overnight at 30°C, postfixed in 4% PFA, and mounted.

Enucleations

P2 and P8 *Isl2*^{tlacZ} mice were anesthetized, one eye was removed, and eyelids closed. Two to eight days later, the remaining eye was injected with CTB-Alexa 594. Wholemount X-gal staining was done as above but for 7 days to ensure maximum staining. Some cases were sectioned then processed for X-gal staining or β-gal immunostaining.

Anterograde Labeling and Quantitation

Mice were anesthetized and eyes filled with 0.5 μl of cholera toxin subunit B (CTB) conjugated to Alexa dyes 488 (green) or 594 (red; Molecular Probes). After 8 hr mice were reanesthetized, perfused with 4% PFA, and sectioned at 100 μm on a vibratome. Quantitative analyses were done with NIH Image and Photoshop as described (Muir-Robinson et al., 2002) on images of four sections covering the largest LGN area. The LGN was cropped and the OT was traced and digitally removed. Each image was intensity normalized in Photoshop using the full intensity spectrum, then imported into NIH Image as a grayscale eight-bit TIF. An average background value was obtained from each normalized image. The "histogram" function in NIH Image generated a pixel and intensity count, further analyzed with Microsoft Excel in two ways: (1) LGN coverage/thresholds, in which the maximum range of thresholds was used: 2×, 3×, 4×, and 5× above background (by 5× above background, signal in wt approached 0). All pixel intensities above threshold were calculated as a percentage of total pixel count. (2) Total intensity, in which the number of pixels at each intensity was multiplied by the actual intensity value of each pixel and summed; intensity levels from background pixels were subtracted from the total to yield signal intensity. In both methods, all four sections were averaged first to obtain a "case average," which was averaged for a "genotype average."

Retrograde Labeling and Quantitation

Multiple injections of 0.1–0.2 μl of rhodamine/fluorescein beads or DiI were made into anterior SC; injections were not made into medial most SC to avoid labeling contralaterally projecting RGCs in ipsilateral retina. After 8 to 24 hr, mice were perfused with PFA; after postfixing, retinas were removed and flat mounted. Two analyses were used: a pixel intensity threshold analysis (an automated method to determine absolute levels of retrograde labeling) and direct cell counts. Data is normalized for slight differences in injection sizes. The pixel intensity threshold analysis was done on digital images of flat-mounted retinas normalized for the full grayscale spectrum using Photoshop, then analyzed for number of pixels with an intensity level above background for equivalent areas across retinas using Image J (NIH image website). Background was subtracted using the rolling ball filter (radius 5; Muir-Robinson et al., 2002). Threshold was adjusted similarly for each image.

Acknowledgments

This work was supported by NEI grant R01 EY07025 (D.M.O'L.). S.L.P. is supported by R01 NS37116. Stipend for W.P. was generously provided by C. Stevens. We thank K. Kearns for technical assistance, M. Feller, T. McLaughlin, and C. Mason for discussions, S. Brown for Zic2 antibody, and M. Henkemeyer for *EphB1* reporter mice.

Received: January 21, 2004
Revised: July 1, 2004
Accepted: September 23, 2004
Published: November 11, 2004

References

Abercrombie, M. (1946). Estimation of nuclear population from microtome sections. Anat. Rec. *94*, 239–247.

Brown, A., Yates, P.A., Burrola, P., Ortuno, D., Vaidya, A., Jessell, T.M., Pfaff, S.L., O'Leary, D.D.M., and Lemke, G. (2000). Topographic mapping from retina to the midbrain is controlled by relative but not absolute levels of EphA receptor signaling. Cell *102*, 77–88.

Brown, L.Y., Kottmann, A.H., and Brown, S. (2003). Immunolocalization of Zic2 expression in the developing mouse forebrain. Gene Expr. Patterns *3*, 361–367.

Colello, R.J., and Guillery, R.W. (1990). The early development of retinal ganglion cells with uncrossed axons in the mouse: retinal position and axonal course. Development *108*, 515–523.

Drager, U.C. (1985). Birth dates of retinal ganglion cells giving rise to the crossed and uncrossed optic projections in the mouse. Proc. R. Soc. Lond. B. Biol. Sci. *224*, 57–77.

Drager, U.C., and Olsen, J.F. (1980). Origins of crossed and uncrossed retinal projections in pigmented and albino mice. J. Comp. Neurol. *191*, 383–412.

Erkman, L., Yates, P.A., McLaughlin, T., McEvilly, R.J., Whisenhunt, T., O'Connell, S.M., Krones, A.L., Kirby, M.A., Rapaport, D.H., Bermingham, J.R., et al. (2000). A POU domain transcription factor-dependent program regulates axon pathfinding in the vertebrate visual system. Neuron *28*, 779–792.

Fukuda, Y., Sawai, H., Watanabe, M., Wakakuwa, K., and Morigiwa, K. (1989). Nasotemporal overlap of crossed and uncrossed retinal ganglion cell projections in the Japanese monkey (Macaca fuscata). J. Neurosci. *9*, 2353–2373.

Godement, P., Salaun, J., and Imbert, M. (1984). Prenatal and postnatal development of retinogeniculate and retinocollicular projections in the mouse. J. Comp. Neurol. *230*, 552–575.

Godement, P., Salaun, J., and Mason, C.A. (1990). Retinal axon pathfinding in the optic chiasm: Divergence of crossed and uncrossed fibers. Neuron *5*, 173–186.

Guillery, R.W., and Herrup, K. (1997). Quantification without pontification: choosing a method for counting objects in sectioned tissues. J. Comp. Neurol. *386*, 2–7.

Herrera, E., Brown, L., Aruga, J., Rachel, R.A., Dolen, G., Mikoshiba, K., Brown, S., and Mason, C.A. (2003). Zic2 patterns binocular vision by specifying the uncrossed retinal projection. Cell *114*, 545–557.

Jessell, T.M. (2000). Neuronal specification in the spinal cord: inductive signals and transcriptional codes. Nat. Rev. Genet. *1*, 20–29.

Marcus, R.C., Blazeski, R., Godement, P., and Mason, C.A. (1995). Retinal axon divergence in the optic chiasm: uncrossed axons di-

verge from crossed axons in a midline glial specialization. J. Neurosci. *15*, 3716–3729.

Marcus, R.C., Matthews, G.A., Gale, N.W., Yancopoulos, G.D., and Mason, C.A. (2000). Axon guidance in the mouse optic chiasm: retinal neurite inhibition by ephrin "A"-expressing hypothalamic cells in vitro. Dev. Biol. *221*, 132–147.

Mason, C.A., and Sretavan, D.W. (1997). Glia, neurons, and axon pathfinding during optic chiasm development. Curr. Opin. Neurobiol. *7*, 647–653.

Muir-Robinson, G., Hwang, B.J., and Feller, M.B. (2002). Retinogeniculate axons undergo eye-specific segregation in the absence of eye-specific layers. J. Neurosci. *22*, 5259–5264.

Nakagawa, S., Brennan, C., Johnson, K.G., Shewan, D., Harris, W.A., and Holt, C.E. (2000). Ephrin-B regulates the ipsilateral routing of retinal axons at the optic chiasm. Neuron *25*, 599–610.

O'Leary, D.D.M., Gerfen, C.R., and Cowan, W.M. (1983). The development and restriction of the ipsilateral retinofugal projection in the chick. Brain Res. *312*, 93–109.

O'Leary, D.D.M., Crespo, D., Fawcett, J.W., and Cowan, W.M. (1986). The effect of intraocular tetrodotoxin on the postnatal reduction in the numbers of optic nerve axons in the rat. Brain Res. *395*, 96–103.

Plump, A.S., Erskine, L., Sabatier, C., Brose, K., Epstein, C.J., Goodman, C.S., Mason, C.A., and Tessier-Lavigne, M. (2002). Slit1 and Slit2 cooperate to prevent premature midline crossing of retinal axons in the mouse visual system. Neuron *33*, 219–232.

Reid, R.C. (2003). Vision. In Fundamentals of Neuroscience, L.R. Squire, F.E. Bloom, S.K. McConnell, J.L. Roberts, N.C. Spitzer, and M.J. Zigmond, eds. (San Diego, CA: Academic Press), pp. 469–498.

Sretavan, D.W. (1990). Specific routing of retinal ganglion cell axons at the mammalian optic chiasm during embryonic development. J. Neurosci. *10*, 1995–2007.

Sretavan, D.W., and Reichardt, L.F. (1993). Time-lapse video analysis of retinal ganglion cell axon pathfinding at the mammalian optic chiasm: Growth cone guidance using intrinsic optic chiasm cues. Neuron *10*, 761–777.

Thaler, J.P., Koo, S.J., Kania, A., Lettieri, K., Andrews, S., Cox, C., Jessell, T.M., and Pfaff, S.L. (2004). A postmitotic role for Isl-class LIM homeodomain proteins in the assignment of visceral spinal motor neuron identity. Neuron *41*, 337–350.

Wang, L.C., Dani, J., Godement, P., Marcus, R.C., and Mason, C.A. (1995). Crossed and uncrossed retinal axons respond differently to cells of the optic chiasm midline in vitro. Neuron *15*, 1349–1364.

Williams, S.E., Mann, F., Erskine, L., Sakurai, T., Wei, S., Rossi, D.J., Gale, N.W., Holt, C.E., Mason, C.A., and Henkemeyer, M. (2003). Ephrin-B2 and EphB1 mediate retinal axon divergence at the optic chiasm. Neuron *39*, 919–935.

Wong, R.O. (1999). Retinal waves and visual system development. Annu. Rev. Neurosci. *22*, 29–47.

Xiang, M. (1998). Requirement for Brn-3b in early differentiation of postmitotic retinal ganglion cell precursors. Dev. Biol. *197*, 155–169.